*Steel and Composite Structures, Vol. 1, No. 4 (2001) 459-480*
DOI: http://dx.doi.org/10.12989/scs.2001.1.4.459


# Seismic response and energy dissipation in partially restrained and fully restrained steel frames: An analytical study

Alfredo Reyes-Salazar†

*Facultad de Ingeniería, Universidad Autónoma de Sinaloa, Culiacán, Sinaloa, México*

Achintya Haldar†

*Department of Civil Engineering and Engineering Mechanics, University of Arizona, Tucson, Arizona, USA*

**Abstract.** The damage suffered by steel structures during the Northridge (1994) and Kobe (1995) earthquakes indicates that the fully restrained (FR) connections in steel frames did not behave as expected. Consequently, researchers began studying other possibilities, including making the connections more flexible, to reduce the risk of damage from seismic loading. Recent experimental and analytical investigations pointed out that the seismic response of steel frames with partially restrained (PR) connections might be superior to that of similar frames with FR connections since the energy dissipation at PR connections could be significant. This beneficial effect has not yet been fully quantified analytically. Thus, the dissipation of energy at PR connections needs to be considered in analytical evaluations, in addition to the dissipation of energy due to viscous damping and at plastic hinges (if they form). An algorithm is developed and verified by the authors to estimate the nonlinear time-domain dynamic response of steel frames with PR connections. The verified algorithm is then used to quantify the major sources of energy dissipation and their effect on the overall structural response in terms of the maximum base shear and the maximum top displacement. The results indicate that the dissipation of energy at PR connections is comparable to that dissipated by viscous damping and at plastic hinges. In general, the maximum total base shear significantly increases with an increase in the connection stiffness. On the other hand, the maximum top lateral displacement $U_{max}$ does not always increase as the connection stiffness decreases. Energy dissipation is considerably influenced by the stiffness of a connection, defined in terms of the $T$ ratio, i.e., the ratio of the moment the connection would have to carry according to beam line theory (Disque 1964) and the fixed end moment of the girder. A connection with a $T$ ratio of at least 0.9 is considered to be fully restrained. The energy dissipation behavior may be quite different for a frame with FR connections with a $T$ ratio of 1.0 compared to when the $T$ ratio is 0.9. Thus, for nonlinear seismic analysis, a $T$ ratio of at least 0.9 should not be considered to be an FR connection. The study quantitatively confirms the general observations made in experimental results for frames with PR connections. Proper consideration of the PR connection stiffness and other dynamic properties are essential to predict dynamic behavior, no matter how difficult the analysis procedure becomes. Any simplified approach may need to be calibrated using this type of detailed analytical study.

**Keywords:** seismic loading; energy dissipation; steel frames; partially restrained; fully restrained; inelastic analysis; connection stiffness; time history analysis; connection parameters.

†Professor

## 1. Introduction

The most recent trend in the profession is to make connections in steel frames flexible to reduce the risk of damage when subjected to seismic loading (Richard *et al*. 1997). Steel frames with partially restrained connections (PR) are not recommended in areas of high seismicity. The reason for this may be the belief that PR frames will undergo excessive deformation when subjected to strong motions. The current design codes do not contain provisions on how to design these systems in seismic zones. For design purposes, beam-to-column connections of steel frames are usually considered to be either fully restrained (FR) or perfectly pinned. Conventional design and analysis methods were developed using these simplified assumptions. However, it is known that the connections in a typical steel frame are essentially partially restrained (PR) with different rigidities. The Load and Resistance Factor Design Specifications published by the American Institute of Steel Construction (AISC 1994), representing the steel fabrication industry, recognize both FR and PR connections. PR connections are expected to be more economical than FR connections since they are much easier to fabricate. However, the conventional analysis and design procedures generally used in the profession and discussed in textbooks cannot be used for frames with PR connections even when the load is small and applied statically, producing small deformation. Nonlinear analysis procedures need to be used. The analysis of steel frames with PR connections for seismic design is even more challenging. Moreover, there is a general feeling that frames with PR connections will undergo larger lateral displacement than frames with FR connections because of their relative flexibility, and consequently the $P$-$\Delta$ phenomenon may be detrimental to the performance of the frames.

In recent experimental and analytical investigations (Nader and Astaneh 1991, Leon and Shin 1995, Elnashai *et al*. 1998), it was pointed out that steel frames with FR connections might not be the optimal solution. Nader and Astaneh observed that the presence of PR connections reduced the lateral stiffness, but increased the energy dissipation capacity at PR connections. Leon and Shin concluded that PR frames presented very stable hysteretic behavior when subjected to cyclic loadings. Elnashani *et al*. showed that the relative deformations in PR frames might be lower than those in FR frames under the same earthquake loading. This is because PR frames have longer periods of vibration and may attract lower inertial forces, and the amount of energy dissipated at PR connection is expected to be greater. In all previous studies, the amount of extra energy dissipation at PR connections was not quantified.

Since the energy dissipation characteristics of steel frames will significantly dictate their dynamic behavior, it is important to estimate the contributions of different sources of energy dissipation and assess their relative significance. This is one of the main objectives of this paper. The effect of connection flexibility on the overall seismic response, in terms of the total base shear, is also explicitly addressed in this study. The base shear is an important parameter in many simplified codified approaches. The intent of the paper is to provide a quantitative interpretation of information that is usually discussed qualitatively or observed experimentally.

## 2. Absorption and dissipation of energy

To meet the objectives of this study, the energy balance concept can be used to quantify various sources of energy absorption and dissipation in nonlinear PR frames under seismic loading. The input energy ($E_I$) of a PR steel frame during time interval $t_1$ to $t_2$ due to seismic loading is absorbed by the

elastic strain energy ($E_S$) and kinetic energy ($E_K$), and dissipated by the hysteretic behavior of the material at the location of plastic hinges ($E_P$), if they form, by viscous damping ($E_D$) and by hysteretic behavior of the PR connections ($E_C$). The concept can be mathematically represented as:

$$E_I = \Delta E_S + \Delta E_K + E_P + E_D + E_C \tag{1}$$

The success in implementing the concept depends how accurately each term in Eq. (1) is evaluated, as elaborated further below.

The input energy for a given inertial force $p_i(t)$ can be calculated as:

$$E_I = \sum_{i=1}^{l} \left( \int_{t_1}^{t_2} p_i(t) \dot{u}_i(t) dt \right) \tag{2}$$

where $l$ is the number of inertial forces acting on the structure, $p_i(t)$ is the $i$th inertial force and $\dot{u}_i$ is the corresponding velocity. The summation is taken to consider all inertial forces acting on the structure.

To evaluate Eq. (2), information is needed on velocity as a function of time at various locations of a structure. As will be discussed later, similar information on displacement and rotation is required to evaluate other terms in Eq. (1). A time-domain nonlinear seismic analysis algorithm considering all major sources of nonlinearity is essential to evaluate all the vectors of displacement, velocity and rotation. The authors and their colleagues developed an efficient finite element-based time nonlinear algorithm (Haldar and Nee 1989, Gao and Haldar 1995, Reyes-Salazar 1997). It cannot be presented here due to lack of space. Only the essential elements of the algorithm are briefly discussed below.

## 3. Nonlinear seismic response analysis

The linear iterative strategy is used to solve the nonlinear dynamic equation of motion as:

$$\boldsymbol{m}^{(t+\Delta t)}\ddot{\boldsymbol{U}}^{(k)} + {}^{t}\boldsymbol{C}^{(t+\Delta t)}\dot{\boldsymbol{U}}^{(k)} + {}^{t}\boldsymbol{K}^{(t+\Delta t)}\Delta\boldsymbol{U}^{(k)} = {}^{(t+\Delta t)}\boldsymbol{F}^{(k)} - {}^{(t+\Delta t)}\boldsymbol{R}^{(k-1)} - \boldsymbol{m}\ddot{\boldsymbol{U}}_g^{(k)} \tag{3}$$

where $\boldsymbol{m}$, $\boldsymbol{C}$ and ${}^{t}\boldsymbol{K}$ are the mass, damping and the tangent stiffness matrixes, respectively. $\ddot{\boldsymbol{U}}$ and $\dot{\boldsymbol{U}}$ are the acceleration and velocity vectors, respectively, $\boldsymbol{\Delta U}$ is the incremental displacement vector, $\boldsymbol{F}$ is the external load vector, $\boldsymbol{R}$ is the internal force vector and $\ddot{\boldsymbol{U}}_g$ is the ground acceleration vector. Superscripts $(t + \Delta t)$ and $(k)$ indicate the time and the iteration number, respectively.

The global mass, tangent stiffness matrixes and internal force vectors are developed by assembling information on all the elements using the standard finite element concept. Explicit expressions for the tangent stiffness matrix and the internal force vector are developed for each beam-column element using the assumed stress-based finite element method for the $k$th iteration at time $t$. The nonlinear elastic tangent stiffness matrix for a beam-column element, $\boldsymbol{K}^e$, can be represented as

$$\boldsymbol{K}^e = \boldsymbol{A}_{\sigma do}^{T} \boldsymbol{A}_{\sigma\sigma}^{-1} \boldsymbol{A}_{\sigma do} + \boldsymbol{A}_{ddo} \tag{4}$$

where $\boldsymbol{A}_{\sigma\sigma}^{-1}$ is the elastic property matrix, $\boldsymbol{A}_{\sigma do}$ is the transformation matrix and $\boldsymbol{A}_{ddo}$ is the geometric stiffness matrix. Similarly, the internal force vector of an element level, $\boldsymbol{R}^e$, can be expressed as

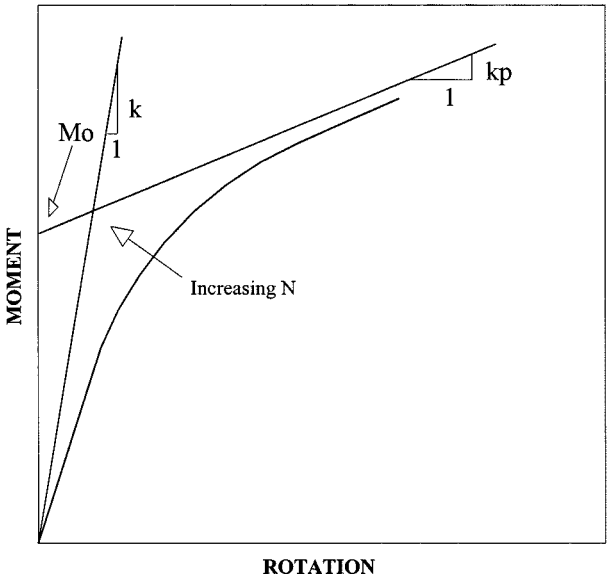


Fig. 1 Parameters of the Richard's model

$$R^e = -\boldsymbol{A}_{\sigma do}^T \boldsymbol{A}_{\sigma\sigma}^{-1} R_\sigma + R_{do} \tag{5}$$

where $\boldsymbol{R}_{do}$ is the homogeneous part of the internal force vector and $\boldsymbol{R}_\sigma$ is the deformation difference vector. It is not possible to give explicit expressions for the terms of Eqs. (4) and (5) due to lack of space, but they can be found in the literature (Gao and Haldar 1995).

The consideration of PR connections is an important part of this study. Connections are structural elements that transmit axial and shear forces, torsion and bending moments between beams and columns. For plane structures, the case addressed in this paper, the torsion effect on connection deformation can be neglected. Furthermore, it has been shown that the effect of shear and axial forces is small in comparison with that of bending moment and can also be neglected. Thus, the bending moment at the connections and the corresponding relative rotation, generally referred to as moment-relative rotation ($M$-$\theta$) curves, are used to represent the flexible behavior of PR connections.

Many alternatives are available in the literature to define $M$-$\theta$ curves to represent the PR connection behavior, i.e., piecewise linear, polynomial, exponential, $B$-spline, and the Richard model. The Richard four-parameter model is used in this study, as shown in Fig. 1. This model is used because of its applicability to a wide variety of connections; it was developed using experimental data.

Using the Richard model (1993), the tangent stiffness $K(\theta)$ of the $M$-$\theta$ curve can be shown to be:

$$K(\theta) = \frac{dM}{d\theta} = \frac{(k - k_p)\theta}{\left[1 + \left|\frac{(k - k_p)\theta}{M_0}\right|^N\right]^{(N+1)/N}} \tag{6}$$

where $k$ is the initial or elastic stiffness, $k_p$ is the plastic stiffness, $M_0$ is the reference moment, and

$N$ is the curve shape parameter, as shown in Fig. 1.

For numerical analysis, a beam-column element is used to represent a PR connection in this study, except that its stiffness needs to be updated continuously depending upon the value of $\theta$ at any point of interest. Thus, to consider the presence of PR connections, the size of the structural stiffness matrix will be increased by the number of PR connections to be included. The tangent stiffness of the structure can still be expressed in explicit form. The only difference is that the stiffness of the beam-column element representing a PR connection needs to be updated at each iteration according to Eq. (6).

The loading part of a PR connection was considered so far. The monotonic loading behavior discussed earlier and the Masing rule (Jayakumar and Beck 1988) are used to theoretically develop the unloading and reloading behavior at the PR connections. Gao and Haldar (1995) showed that when the connection element is unloading and reloading, the tangent stiffness could be calculated as:

$$K(\theta) = \frac{(k - k_p)}{\left[1 + \left|\frac{(k - k_p)(\theta_a - \theta)}{2M_0}\right|^N\right]^{(N+1)/N}} + k_p \tag{7}$$

where $\theta_a$ is the relative rotation of the PR connection at the load reversal point. Thus, considering loading, unloading and reloading, the appropriate tangent stiffness for each of the PR connections can be used to formulate the overall structural stiffness matrix.

Thus far the nonlinear structural behavior produced by the PR connections has been discussed. The algorithm needs to be modified to also consider material nonlinearity if the excitation level is relatively large. In this study, the material is considered to be elasto-plastic. Concentrated plasticity behavior is assumed at plastic hinge locations. For mathematical modeling, plastic hinges are assumed to occur at locations where the combined action of axial force, torsional and bending moments satisfy a prescribed yield function. This is discussed in detail elsewhere by Gao and Haldar (1995). For plane structures, the case addressed in this study, the yield function has the following general form:

$$f(A, M, \sigma_y) = 0 \quad \text{at} \quad X = l_p \tag{8}$$

where $A$ is the axial force, $M$ is the bending moment, $\sigma_y$ is the yield stress, and $l_p$ is the location of the plastic hinge.

The presence of plastic hinges in the structure will produce additional axial deformation and relative rotation in a particular element. Thus, the tangent stiffness matrix needs to be modified if plastic hinges form. The elasto-plastic tangent stiffness matrix $\boldsymbol{K_P}$ and the elasto-plastic internal force vector $\boldsymbol{R_P}$ can be obtained by modifying the corresponding elastic matrixes as (Shi and Atluri 1988, Haldar and Nee 1989):

$$\boldsymbol{K_P^e} = \boldsymbol{K^e} - \boldsymbol{A_{\sigma do}^T A_{\sigma\sigma}^{-1} V_P C_P^T A_{\sigma do}} \tag{9}$$

and

$$\boldsymbol{R_P^e} = \boldsymbol{A_{\sigma do}^T (A_{\sigma\sigma}^{-1} V_P C_P^T - A_{\sigma\sigma}^{-1})\hat{R}_\sigma + R_{do}} \tag{10}$$

All the parameters in Eqs. (9) and (10) except $\boldsymbol{V_P}$ and $\boldsymbol{C_P}$ were defined earlier. $\boldsymbol{V_P}$ and $\boldsymbol{C_P}$ can be shown to be:

$$\boldsymbol{V_P} = \left[\frac{-\partial \boldsymbol{f}}{\partial \boldsymbol{N}}, \quad \frac{-\partial \boldsymbol{f}}{\partial \boldsymbol{M}}(1-\boldsymbol{X}/1), \quad \frac{-\partial \boldsymbol{f}}{\partial \boldsymbol{M}}(\boldsymbol{X}/1)\right]^{\boldsymbol{T}} \tag{11}$$

$$\boldsymbol{C_P^T} = (\boldsymbol{V_P^T A_{\sigma\sigma}^{-1}})^{-1} \boldsymbol{V_P^{-1}} \boldsymbol{A_{\sigma\sigma}^{-1}} \tag{12}$$

and

$$\hat{\boldsymbol{R}}_\sigma = \boldsymbol{R}_\sigma + \begin{Bmatrix} H_p \\ \theta_p^*(1-X/l) \\ \theta_p^*(X/l) \end{Bmatrix} \tag{13}$$

In Eq. (13) $H_p$ and $\theta_p$* are the additional axial elongation and additional relative rotation due to plastic hinges. All the other parameters were discussed earlier.

Depending on the level of earthquake excitation, all the elements in a typical structure may remain elastic, or some of the elements may remain elastic and the rest may yield. As stated earlier, the structural stiffness matrix can be explicitly obtained by considering individual elements and the corresponding element stiffness matrixes, depending on the particular state they are in. If a particular element is in an elastic state, Eqs. (4) and (5) are used. If the element has yielded, Eqs. (9) and (10) should be used instead.

The only other information required to solve Eq. (3) is the damping. Dissipation of energy by damping takes place throughout the total excitation time and is present even for small deformations of the structure. Based on an extensive literature review, it is observed that the following Rayleigh-type damping is very commonly used in the profession:

$$\boldsymbol{C} = \alpha \boldsymbol{m} + \gamma\, {}^t\boldsymbol{K} \tag{14}$$

where $\alpha$ and $\gamma$ are the proportional constants. The use of both the tangent stiffness and the mass matrices is a rational approach to estimate the energy dissipated by viscous damping in a nonlinear seismic analysis. The constants $\alpha$ and $\gamma$ can be determined from specified damping ratios $\xi_i$ and $\xi_j$ for the *i*th and *j*th modes, respectively. Then the following algebraic equation system is solved for $\alpha$ and $\gamma$ (Clough and Penzien 1993):

$$\frac{1}{2}\begin{vmatrix} \frac{1}{\omega_i} & \omega_i \\ \frac{1}{\omega_j} & \omega_j \end{vmatrix} \begin{vmatrix} \alpha \\ \gamma \end{vmatrix} = \begin{vmatrix} \xi_i \\ \xi_j \end{vmatrix} \tag{15}$$

where $\omega_i$ and $\omega_j$ are the natural frequencies of the *i*th and *j*th mode, respectively, and are calculated using the Stodola method in this study. Usually the *i*th mode is selected as the first mode, and the *j*th mode as the higher mode that contributes significantly to the structural response.

It is clear that a nonlinear time-domain seismic response algorithm can be developed considering geometric and material nonlinearity and the flexibility of the PR connections. The algorithm needs to be verified at this stage.

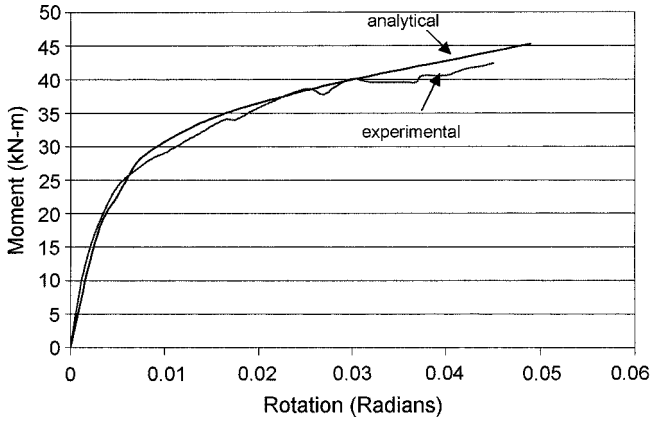


Fig. 2 Experimental and analytical $M$-$\sigma$ curve

## 4. Verification of the analytical model

The mathematical model is verified by using a steel frame experimentally investigated by Leon and Shin (1995). It is a two-story two-bay frame. The span of each bay is 4.06 m, and the story height is 1.88 m. W6×20 wide flange section is used for the exterior columns, and W6×25 is used for the interior columns. All beams are made of W8×18. All members are made of A36 steel. All connections consist of top and seat angles (L6×3 1/2×5/16) and web angles (2L3 1/2×2 1/2×1/4) and are made from A36 steel. The frame is assumed to be fixed at the base. This test was conducted in a load-control mode and the drift of the frame was measured. See Leon and Shin (1995) for further details on the frame, the connections and the experiment.

All the connections are considered to be PR, and are represented by the Richard model. The experimental $M$-$\sigma$ curve for the connections reported by Leon and Shin and the analytical $M$-$\sigma$ curve

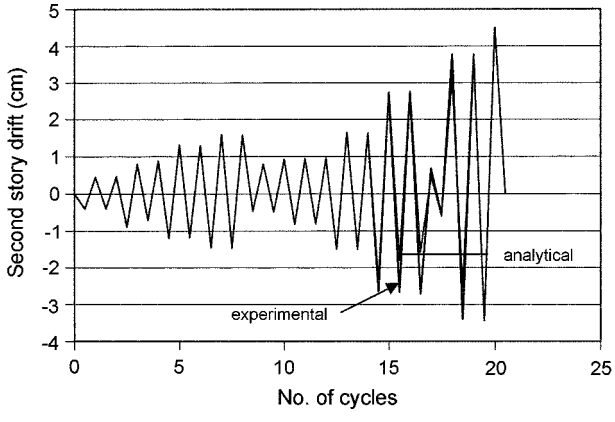


Fig. 3 Experimental and analytical story drift

represented by the Richard model are shown in Fig. 2. It is observed that both curves match very well.

In this study, the connection rigidity is defined in terms of the *T* ratio. It is the ratio of the moment the connection would have to carry according to the beam line theory (Disque 1964) and the fixed end moment of the girder. A *T* ratio greater than 0.9 generally represents a fully restrained connection. Using the Richard curve, the *T* ratio for the connections is found to be 0.3, representing a very flexible connection.

Leon and Shin (1995) reported the experimental results of the second story drift as shown in Fig. 3. The analytical results obtained from the model considered in this study are also shown in Fig. 3. A reasonable agreement between the experimental and theoretical results can be observed. Thus, the theoretical model used in this study appears to be reasonable for estimating the nonlinear time domain dynamic response of steel frames with PR connections. This verified algorithm is used to estimate all the components of energy absorption and dissipation as discussed below.

## 5. Evaluations of absorption and dissipation of energy

The first component of energy absorption, i.e., the variation in the elastic strain energy, can be calculated as (Uang and Bertero 1990):

$$\Delta E_S = \left(\frac{1}{2}\boldsymbol{U}^T\,{}^t\boldsymbol{K}\boldsymbol{U}\right)_{t_2} - \left(\frac{1}{2}\boldsymbol{U}^T\,{}^t\boldsymbol{K}\boldsymbol{U}\right)_{t_1} \tag{16}$$

The tangent stiffness matrix ${}^t\boldsymbol{K}$ and the displacement vector $\boldsymbol{U}$ can be calculated using the algorithm discussed earlier. The variation in the kinetic energy is obtained as (Uang and Bertero 1990):

$$\Delta \boldsymbol{E_k} = \left(\frac{1}{2}\dot{\boldsymbol{U}}^T\boldsymbol{m}\dot{\boldsymbol{U}}\right)_{t_2} - \left(\frac{1}{2}\dot{\boldsymbol{U}}^T\boldsymbol{m}\dot{\boldsymbol{U}}\right)_{t_1} \tag{17}$$

Once the yield function is satisfied, a plastic hinge forms and the energy dissipation process begins at that location. The plastic energy at plastic hinges can be estimated by calculating the work done by the resultant stresses through the corresponding plastic deformations. For plane frames it can be expressed as (Haldar and Nee 1989):

$$E_P = \sum_{i=1}^{q} M_{P_i}[(\theta_{P_i})_{t_2} - (\theta_{P_i})_{t_1}] + \sum_{i=1}^{q} P_{P_i}[(H_{P_i})_{t_2} - (H_{P_i})_{t_1}] \tag{18}$$

where $q$ is the number of plastic hinges, $M_{P_i}$ and $P_{P_i}$ are the moment and axial force, respectively, acting on the $i$th plastic hinge, and $\theta_{P_i}$ and $H_{P_i}$ are the corresponding plastic rotation and plastic axial elongation, respectively. The summation sign is taken to consider the contributions of all plastic hinges developed in the structure.

The energy dissipated by viscous damping is estimated as:

$$E_D = \int_{t_1}^{t_2} (\dot{\boldsymbol{U}}^T\boldsymbol{C}\dot{\boldsymbol{U}})\,dt \tag{19}$$

where $\boldsymbol{C}$ is the damping matrix of the structure.

The dissipation of energy at PR connections ($E_C$) is estimated by considering the hysteretic behavior of bending moment, shear and axial forces. However, it has been shown (Reyes-Salazar and Haldar 2000) that the energy dissipation due to shear and axial forces is negligible compared to that due to bending moment. This is because the shear and axial forces deformation behaviors are virtually linear, and the corresponding energy dissipation due to hysteretic behavior can be neglected. Therefore, only the energy dissipation due to bending moment at PR connections is reported in this paper. $E_C$ is quantified as

$$E_C = \sum_{j=1}^{s}\left(\int_{\theta_1}^{\theta_2} M_j d\theta_j\right) = \sum_{j=1}^{s}\left(\int_{t_1}^{t_2} M_j \dot{\theta}_j dt_j\right) \tag{20}$$

where $s$ is the number of PR connections in the structure, and $M_j$ and $\theta_j$ are the moment and relative rotation, respectively, at the $j$th connection. The summation is taken to consider the contributions of all the connections in the structure.

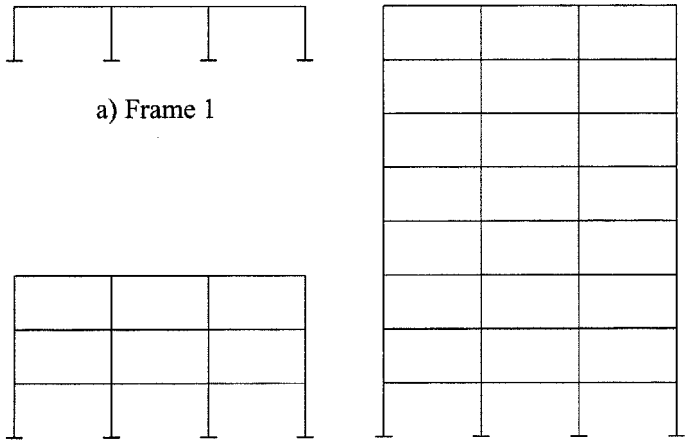


Fig. 4 Geometry of the structural models

Table 1 Member sizes

| Frame | Story | Ext. Columns | Int. Columns | Girders |
|---|---|---|---|---|
| 1 | 1 | W14×48 | W14×68 | W18×40 |
| 2 | 1 | W14×68 | W14×99 | W18×55 |
| | 2-3 | W14×48 | W14×68 | W18×40 |
| 3 | 1-2 | W14×99 | W24×131 | W24×68 |
| | 3-4 | W14×90 | W24×94 | W24×55 |
| | 5-6 | W14×74 | W24×84 | W21×50 |
| | 7-8 | W14×48 | W24×55 | W18×40 |

## 6. Numerical results

### 6.1. Structural models and earthquakes

To estimate the dissipation of energy due to each of the sources mentioned earlier, three steel frames representing different dynamic characteristics are considered. They are denoted hereafter as Frames 1 through 3. The geometry of these frames is shown in Fig. 4 and the member sizes in Table 1. Their fundamental periods with FR connections are 0.32, 1.52 and 3.4 sec, respectively, representing frames with short, intermediate and large periods. Frame 1 is a one-story three-bay frame. Its bay width is 7.32 m and the story height is 3.66 m. The geometry of Frames 2 and 3 are similar to that of Frame 1, except that they are three-story and eight-story buildings, respectively. Frames 2 and 3 were used by Roeder *et al*. (1993) in their analytical studies. In all these frames the weight of each story is considered to be 253,440 kg.

Nine recorded time histories are used to excite these frames. The first one is the El Centro Earthquake of 1940, the second one is the Mexico City Earthquake of 1985, and the other seven were recorded during the Northridge Earthquake of 1994 at the following stations: Santa Susana, Canoga Park; 4929 Wilshire Boulevard, Los Angeles; 1525 Ventura Boulevard, Sherman Oaks; Topanga Fire Station; 4929 Wilshire Boulevard, Los Angeles; 10660 Wilshire Boulevard, Los Angeles, and 10751 Wilshire Boulevard, Los Angeles. These earthquakes are denoted hereafter as Earthquakes 1 through 9. They are selected to represent many different characteristics of strong

Table 2 Connections' parameters

| Frame | Story | $T$ = 0.3 | | | | $T$ = 0.6 | | | |
|---|---|---|---|---|---|---|---|---|---|
| | | $K(10^5)$ (kN-m/rad) | $K_P$ (kN-m/rad) | $M_0$ ($10^2$) (kN-m) | $N$ | $K$ ($10^5$) (kN-m/rad) | $K_P$ (kN-m/rad) | $M_0$ ($10^2$) (kN-m) | $N$ |
| 1 | 1 | 0.2904 | 1,397.0190 | 0.7209 | 2.70 | 1.1560 | 3,349.6590 | 1.6193 | 2.10 |
| 2 | 1 | 0.3763 | 1,669.3490 | 1.1232 | 2.80 | 1.2543 | 3,777.5900 | 2.4713 | 2.10 |
| | 2-3 | 0.2904 | 1,397.0190 | 0.7209 | 2.70 | 1.1560 | 3,349.6590 | 1.6193 | 2.10 |
| 3 | 1-2 | 1.9504 | 3,646.8490 | 1.8306 | 1.10 | 5.3065 | 7,979.7210 | 4.0917 | 1.10 |
| | 3-4 | 1.5775 | 3,446.6130 | 1.2125 | 1.50 | 3.4205 | 5,865.7170 | 3.1640 | 1.10 |
| | 5-6 | 0.8034 | 2,417.0700 | 1.0034 | 2.20 | 1.7108 | 3,836.3500 | 2.5233 | 1.90 |
| | 7-8 | 0.2904 | 1,397.0190 | 0.7209 | 2.70 | 1.1560 | 3,349.6590 | 1.6193 | 2.10 |

| Frame | Story | $T$ = 0.9 | | | |
|---|---|---|---|---|---|
| | | $K$ ($10^5$) (kN-m/rad) | $K_P$ (kN-m/rad) | $M_0$ ($10^2$) (kN-m) | $N$ |
| 1 | 1 | 2.1255 | 0.4509 | 3.2216 | 2.30 |
| 2 | 1 | 5.5404 | 117.4070 | 5.5856 | 1.10 |
| | 2-3 | 2.1255 | 0.4509 | 3.2216 | 2.30 |
| 3 | 1-2 | 12.8153 | 122.4920 | 8.7745 | 1.10 |
| | 3-4 | 8.7948 | 4.2838 | 5.4703 | 1.60 |
| | 5-6 | 5.7596 | 6.2873 | 4.6590 | 1.60 |
| | 7-8 | 2.1255 | 0.4509 | 3.2216 | 2.30 |

Table 3 Energy dissipation for Frame 1 and $T$ = 0.3

| Earth. (1) | $\xi$ (%) (2) | $U_{max}$ (cm) (3) | $E_C$ (N-m) (4) | $E_D$ (N-m) (5) | $R_1$(%) (6) |
|---|---|---|---|---|---|
| 1 | 1 | 2.95 | 11,561 | 5,736 | 201.6 |
| | 2 | 2.79 | 9,028 | 8,896 | 101.5 |
| | 5 | 2.46 | 5,512 | 13,440 | 41.0 |
| | 10 | 2.03 | 2,467 | 15,970 | 15.5 |
| 2 | 1 | 2.16 | 1,411 | 200 | 705.4 |
| | 2 | 2.06 | 1,088 | 1,006 | 108.1 |
| | 5 | 1.98 | 793 | 2,765 | 28.7 |
| | 10 | 1.68 | 658 | 4,404 | 14.0 |
| 3 | 1 | 2.79 | 21,251 | 7,090 | 299.7 |
| | 2 | 2.67 | 16,731 | 11,528 | 145.1 |
| | 5 | 2.26 | 9,006 | 17,684 | 50.9 |
| | 10 | 1.80 | 3,663 | 21,314 | 17.2 |
| 4 | 1 | 2.49 | 3,488 | 910 | 382.0 |
| | 2 | 2.44 | 2,945 | 1,967 | 149.7 |
| | 5 | 2.31 | 2,522 | 4,565 | 55.3 |
| | 10 | 2.11 | 1,899 | 8,095 | 23.5 |
| 5 | 1 | 2.59 | 11,728 | 5,672 | 206.8 |
| | 2 | 2.49 | 9,529 | 8,297 | 114.8 |
| | 5 | 2.18 | 4,751 | 12,756 | 37.3 |
| | 10 | 1.78 | 1,606 | 13,893 | 11.6 |
| 6 | 1 | 2.29 | 10,518 | 5,675 | 185.3 |
| | 2 | 2.13 | 7,503 | 7,945 | 94.4 |
| | 5 | 1.75 | 2,771 | 10,750 | 25.8 |
| | 10 | 1.32 | 613 | 11,041 | 5.6 |
| 7 | 1 | 2.46 | 11,465 | 6,258 | 183.2 |
| | 2 | 2.41 | 9,250 | 8,937 | 103.5 |
| | 5 | 2.13 | 4,935 | 14,104 | 34.0 |
| | 10 | 1.80 | 2,190 | 18,586 | 11.8 |
| 8 | 1 | 2.79 | 24,869 | 12,656 | 196.5 |
| | 2 | 2.62 | 11,742 | 24,411 | 48.1 |
| | 5 | 2.18 | 10,045 | 22,251 | 45.1 |
| | 10 | 1.68 | 2,767 | 22,997 | 12.0 |
| 9 | 1 | 2.31 | 19,458 | 9,659 | 201.5 |
| | 2 | 2.13 | 13,671 | 13,624 | 100.3 |
| | 5 | 1.88 | 1,739 | 23,288 | 7.5 |
| | 10 | 1.75 | 899 | 20,405 | 4.4 |

motion earthquakes. Additional information on the earthquakes can be obtained from Reyes-Salazar (1997).

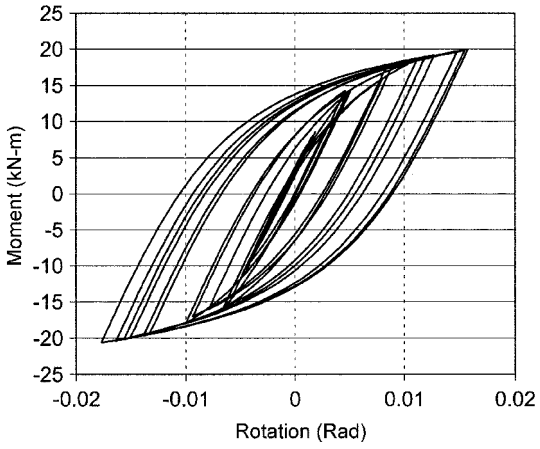


Fig. 5 Moment-rotation curve, Earthquake 2, $T$ = 0.3 and 2% damping

### 6.2. Results and observations

The energy dissipation due to each source discussed earlier is estimated. To make the observations meaningful, the intensity of the earthquakes, viscous damping $\xi$ (expressed in terms of percent of critical damping) and the $T$ ratio are selected for the parametric study. If actual time histories were used, in some cases the frames would develop only very small deformations, and in other cases the frames would collapse, indicating the presence of different levels of nonlinearity. The lateral deformation is a very important serviceability design criterion for seismic loading. To evaluate and compare the different sources of energy dissipation and base shear meaningfully, each earthquake is scaled up or down to produce similar levels of deformation. This will ensure similar levels of nonlinearity in the frame. The maximum interstory displacement developed in each frame ranges between 0.8 and 1.3 percent of the story height for a $T$ ratio of 0.3 and $\xi$ = 2%. Then, these scale factors are kept the same for other damping and $T$ ratios. PR connections with $T$ ratios of 0.3, 0.6, and 0.9 are used for each frame. The Richard parameters for these connections are given in Table 2. Damping values for the first two modes (required to evaluate Eq. 15) are assumed to be the same. It is assumed to be 1, 2, 5 and 10% of critical damping for the parametric study.

All terms in Eq. (1) are calculated for each combination of the parameters. $U_{\max}$, $E_D$, $E_C$ and $E_P$ (if plastic hinges form) are specifically considered in this paper. The fundamental period of the frame with a $T$ ratio of 0.3 is found to be 0.49 sec. The results for Frame 1 excited by the nine earthquakes for $\xi$ = 1, 2, 5 and 10% and a $T$ ratio of 0.3 are summarized in Table 3. The frame did not develop any plastic hinges, and thus $E_P$ cannot be calculated and is not shown in Table 3.

To study the significance of energy dissipation at PR connections relative to that due to viscous damping, a parameter $R_1$ is introduced. It is calculated as $R_1 = (E_C / E_D) \times 100$ and is also shown in Table 3. From the results given in Table 3, several observations can be made. As expected, for a given earthquake, $U_{\max}$ and $E_C$ decrease and $E_D$ increases with an increase in the damping values. The $R_1$ values are large, particularly for low damping values, indicating that the dissipation of energy at PR connections is comparable and sometimes greater than that from viscous damping. The $R_1$ values decrease as damping increases. This is because the rotation of the connections, and consequently $E_C$,

Table 4 Energy dissipation for Frame 1 and $T = 0.6$

| Earth. (1) | $\xi$ (%) (2) | $U_{max}$ (cm) (3) | $E_P$ (N-m) (4) | $E_C$ (N-m) (5) | $E_D$ (N-m) (6) | $R_1$ (%) (7) | $R_2$(%) (8) | $R_3$(%) (9) |
|---|---|---|---|---|---|---|---|---|
| 1 | 1 | 2.97 | 3,068 | 11,692 | 7,828 | 149.4 | 381.1 | 39.2 |
| | 2 | 2.34 | * | 5,946 | 14,621 | 40.7 | * | * |
| | 5 | 1.83 | * | 1,267 | 16,195 | 7.8 | * | * |
| | 10 | 1.35 | * | 322 | 15,188 | 2.1 | * | * |
| 2 | 1 | 1.96 | * | 319 | 742 | 42.0 | * | * |
| | 2 | 1.73 | * | 172 | 1,188 | 14.5 | * | * |
| | 5 | 1.45 | * | 80 | 2,038 | 3.9 | * | * |
| | 10 | 1.27 | * | 64 | 3,116 | 2.1 | * | * |
| 3 | 1 | 2.72 | 4,053 | 8,717 | 4,627 | 188.4 | 215.0 | 87.6 |
| | 2 | 2.54 | 811 | 5,011 | 12,467 | 40.2 | 617.8 | 6.5 |
| | 5 | 2.03 | * | 1,783 | 15,883 | 11.2 | * | * |
| | 10 | 1.50 | * | 448 | 16,316 | 2.8 | * | * |
| 4 | 1 | 2.03 | * | 744 | 1,099 | 67.7 | * | * |
| | 2 | 1.91 | * | 549 | 2,561 | 21.5 | * | * |
| | 5 | 1.80 | * | 307 | 5,033 | 6.1 | * | * |
| | 10 | 1.63 | * | 262 | 7,601 | 3.5 | * | * |
| 5 | 1 | 3.10 | 4,693 | 4,552 | 2,731 | 166.7 | 97.0 | 171.8 |
| | 2 | 2.74 | 1,494 | 4,471 | 6,286 | 71.1 | 299.3 | 23.8 |
| | 5 | 2.24 | * | 1,555 | 11,817 | 13.2 | * | * |
| | 10 | 1.65 | * | 341 | 12,513 | 2.7 | * | * |
| 6 | 1 | 1.37 | * | 779 | 2,738 | 28.5 | * | * |
| | 2 | 1.37 | * | 452 | 4,442 | 10.2 | * | * |
| | 5 | 1.27 | * | 206 | 6,750 | 3.1 | * | * |
| | 10 | 1.02 | * | 82 | 8,464 | 1.0 | * | * |
| 7 | 1 | 2.79 | 2,665 | 7,762 | 8,389 | 92.5 | 291.2 | 31.8 |
| | 2 | 2.62 | 824 | 4,614 | 13,864 | 33.3 | 559.9 | 5.9 |
| | 5 | 2.16 | * | 1,753 | 18,100 | 9.7 | * | * |
| | 10 | 1.55 | * | 425 | 18,641 | 2.3 | * | * |
| 8 | 1 | 1.57 | * | 1,225 | 3,793 | 32.3 | * | * |
| | 2 | 1.55 | * | 992 | 6,297 | 15.8 | * | * |
| | 5 | 1.42 | * | 614 | 11,064 | 5.6 | * | * |
| | 10 | 1.19 | * | 227 | 13,845 | 1.7 | * | * |
| 9 | 1 | 2.18 | * | 2,831 | 7,337 | 38.6 | * | * |
| | 2 | 2.06 | * | 1,815 | 9,291 | 19.5 | * | * |
| | 5 | 1.70 | * | 823 | 13,312 | 6.2 | * | * |
| | 10 | 1.42 | * | 365 | 16,492 | 2.2 | * | * |

* = no plastic hinge was developed

also decreases as damping increases. Thus, large deformation of the frame is necessary to produce significant energy dissipation at PR connections. It can also be observed from Table 3 that even though

Table 5 Energy dissipation for Frame 1 and $T$ = 0.9

| Earth. (1) | $\xi$ (%) (2) | $U_{max}$ (cm) (3) | $E_P$ (N-m) (4) | $E_C$ (N-m) (5) | $E_D$ (N-m) (6) | $R_1$ (%) (7) | $R_2$ (%) (8) | $R_3$ (%) (9) |
|---|---|---|---|---|---|---|---|---|
| 1 | 1 | 2.21 | * | 1,100 | 10,096 | 10.9 | * | * |
| | 2 | 1.88 | * | 443 | 12,661 | 3.5 | * | * |
| | 5 | 1.55 | * | 98 | 14,780 | 0.7 | * | * |
| | 10 | 1.24 | * | 29 | 14,499 | 0.2 | * | * |
| 2 | 1 | 1.47 | * | 31 | 584 | 5.5 | * | * |
| | 2 | 1.45 | * | 23 | 1,021 | 2.3 | * | * |
| | 5 | 1.30 | * | 9 | 1,913 | 0.5 | * | * |
| | 10 | 1.22 | * | 6 | 2,888 | 0.2 | * | * |
| 3 | 1 | ** | ** | ** | ** | ** | ** | ** |
| | 2 | 3.30 | 10,849 | 1,719 | 10,572 | 16.3 | 15.9 | 102.6 |
| | 5 | 2.01 | * | 211 | 17,347 | 1.2 | * | * |
| | 10 | 1.42 | * | 43 | 15,664 | 0.3 | * | * |
| 4 | 1 | 2.11 | * | 167 | 913 | 18.3 | * | * |
| | 2 | 1.88 | * | 98 | 2,963 | 3.3 | * | * |
| | 5 | 1.70 | * | 40 | 5,510 | 0.7 | * | * |
| | 10 | 1.52 | * | 23 | 5,432 | 0.4 | * | * |
| 5 | 1 | ** | ** | ** | ** | ** | ** | ** |
| | 2 | 2.79 | 3,756 | 698 | 4,726 | 14.8 | 18.6 | 79.5 |
| | 5 | 2.18 | * | 156 | 11,522 | 1.4 | * | * |
| | 10 | 1.57 | * | 33 | 12,086 | 0.3 | * | * |
| 6 | 1 | 1.68 | * | 172 | 3,167 | 5.4 | * | * |
| | 2 | 1.47 | * | 60 | 4,470 | 1.4 | * | * |
| | 5 | 1.22 | * | 19 | 6,203 | 0.3 | * | * |
| | 10 | 0.97 | * | 8 | 8,072 | 0.1 | * | * |
| 7 | 1 | 2.97 | 9,200 | 1,433 | 1885 | 76.0 | 15.6 | 488.0 |
| | 2 | 3.00 | 4,169 | 1,075 | 9,588 | 11.2 | 25.8 | 43.5 |
| | 5 | 2.13 | * | 212 | 20,120 | 1.1 | * | * |
| | 10 | 1.47 | * | 7 | 19,052 | 0.0 | * | * |
| 8 | 1 | 1.78 | * | 183 | 3,103 | 5.9 | * | * |
| | 2 | 1.50 | * | 91 | 4,979 | 1.8 | * | * |
| | 5 | 1.27 | * | 47 | 8,894 | 0.5 | * | * |
| | 10 | 1.09 | * | 20 | 11,998 | 0.2 | * | * |
| 9 | 1 | 1.75 | * | 270 | 5,849 | 4.6 | * | * |
| | 2 | 1.75 | * | 231 | 8,641 | 2.7 | * | * |
| | 5 | 1.57 | * | 145 | 12,871 | 1.1 | * | * |
| | 10 | 1.32 | * | 88 | 15,694 | 0.6 | * | * |

* = no plastic hinge was developed
** = developed large lateral displacement

Table 6 Energy dissipation for Frame 1 and FR connections

| Earth. (1) | $\xi$ (%) (2) | $U_{max}$ (cm) (3) | $E_P$ (N-m) (4) | $E_D$ (N-m) (5) | $R_3$ (%) (6) |
|---|---|---|---|---|---|
| 1 | 1 | 1.96 | * | 6,293 | * |
| | 2 | 1.68 | * | 9,375 | * |
| | 5 | 1.32 | * | 12,675 | * |
| | 10 | 1.12 | * | 13,416 | * |
| 2 | 1 | ** | ** | ** | ** |
| | 2 | 1.19 | * | 536 | * |
| | 5 | 1.19 | * | 1,626 | * |
| | 10 | 1.17 | * | 2,644 | * |
| 3 | 1 | ** | ** | ** | ** |
| | 2 | 2.90 | 10,803 | 7,099 | 152.2 |
| | 5 | 1.88 | * | 16,076 | * |
| | 10 | 1.30 | * | 14,501 | * |
| 4 | 1 | 2.24 | * | 2,599 | * |
| | 2 | 1.88 | * | 3,773 | * |
| | 5 | 1.60 | * | 5,668 | * |
| | 10 | 1.40 | * | 7,785 | * |
| 5 | 1 | ** | ** | ** | ** |
| | 2 | 2.59 | 2,045 | 7,672 | 26.7 |
| | 5 | 2.03 | * | 11,640 | * |
| | 10 | 1.47 | * | 11,651 | * |
| 6 | 1 | 1.52 | * | 3,555 | * |
| | 2 | 1.37 | * | 4,278 | * |
| | 5 | 1.14 | * | 5,672 | * |
| | 10 | 0.94 | * | 7,744 | * |
| 7 | 1 | ** | ** | ** | ** |
| | 2 | 2.69 | 5,613 | 19,435 | 28.9 |
| | 5 | 2.01 | * | 23,116 | * |
| | 10 | 1.37 | * | 19,082 | * |
| 8 | 1 | 1.30 | * | 2,851 | * |
| | 2 | 1.22 | * | 4,322 | * |
| | 5 | 1.09 | * | 7,462 | * |
| | 10 | 0.97 | * | 10,320 | * |
| 9 | 1 | 2.08 | * | 9,636 | * |
| | 2 | 1.75 | * | 10,946 | * |
| | 5 | 1.45 | * | 12,843 | * |
| | 10 | 1.22 | * | 14,930 | * |

* = no plastic hinge was developed
** = developed large lateral displacement

Table 7 Base shear for Frame 1 and different connection stiffness

| Earth (1) | $\xi$ (%) (2) | $V_3$ (kN) (3) | $V_6$ (kN) (4) | $V_9$ (kN) (5) | $V_{FRC}$ (kN) (6) | $R_4$ (%) (7) | $R_5$ (%) (8) | $R_6$ (%) (9) |
|---|---|---|---|---|---|---|---|---|
| 1 | 1 | 547 | 725 | 667 | 627 | 32.5 | 22.0 | 14.6 |
| | 2 | 525 | 671 | 569 | 538 | 28.0 | 8.5 | 2.5 |
| | 5 | 480 | 516 | 471 | 422 | 7.4 | -1.9 | -12.0 |
| | 10 | 427 | 382 | 378 | 356 | -10.4 | -11.5 | -16.7 |
| 2 | 1 | 489 | 556 | 449 | 418 | 13.6 | -8.2 | -14.6 |
| | 2 | 480 | 498 | 440 | 382 | 3.7 | -8.3 | -20.4 |
| | 5 | 453 | 418 | 391 | 378 | -7.8 | -13.7 | -16.7 |
| | 10 | 409 | 369 | 369 | 369 | -9.8 | -9.8 | -9.8 |
| 3 | 1 | 538 | 743 | ** | ** | 38.0 | ** | ** |
| | 2 | 520 | 698 | 841 | 849 | 34.2 | 61.5 | 63.3 |
| | 5 | 458 | 560 | 609 | 600 | 22.3 | 33.0 | 31.1 |
| | 10 | 387 | 427 | 431 | 409 | 10.3 | 11.5 | 5.8 |
| 4 | 1 | 507 | 565 | 645 | 712 | 11.4 | 27.2 | 40.4 |
| | 2 | 498 | 542 | 574 | 600 | 8.9 | 15.2 | 20.5 |
| | 5 | 480 | 516 | 516 | 507 | 7.4 | 7.4 | 5.6 |
| | 10 | 453 | 467 | 462 | 449 | 2.9 | 2.0 | -1.0 |
| 5 | 1 | 511 | 783 | ** | ** | 53.0 | ** | ** |
| | 2 | 493 | 738 | 787 | 778 | 49.6 | 59.5 | 57.7 |
| | 5 | 449 | 614 | 658 | 645 | 36.6 | 46.5 | 43.6 |
| | 10 | 387 | 467 | 480 | 467 | 20.7 | 24.1 | 20.7 |
| 6 | 1 | 453 | 396 | 507 | 489 | -12.8 | 11.8 | 7.8 |
| | 2 | 431 | 396 | 449 | 440 | -8.3 | 4.1 | 2.1 |
| | 5 | 378 | 364 | 369 | 369 | -3.5 | -2.4 | -2.4 |
| | 10 | 302 | 298 | 271 | 302 | -1.5 | -10.3 | 0.0 |
| 7 | 1 | 476 | 760 | 832 | ** | 59.8 | 74.8 | ** |
| | 2 | 467 | 725 | 809 | 814 | 55.2 | 73.3 | 74.3 |
| | 5 | 427 | 596 | 645 | 636 | 39.6 | 51.0 | 49.0 |
| | 10 | 382 | 445 | 449 | 440 | 16.3 | 17.4 | 15.1 |
| 8 | 1 | 538 | 449 | 534 | 413 | -16.5 | -0.8 | -23.1 |
| | 2 | 511 | 445 | 453 | 387 | -13.0 | -11.3 | -24.4 |
| | 5 | 453 | 409 | 382 | 351 | -9.8 | -15.7 | -22.6 |
| | 10 | 369 | 347 | 329 | 307 | -6.0 | -10.8 | -16.9 |
| 9 | 1 | 476 | 591 | 534 | 663 | 24.3 | 12.2 | 39.3 |
| | 2 | 458 | 560 | 529 | 560 | 22.3 | 15.5 | 22.3 |
| | 5 | 436 | 476 | 480 | 462 | 9.2 | 10.2 | 6.1 |
| | 10 | 418 | 409 | 400 | 387 | -2.1 | -4.3 | -7.5 |

** = developed large lateral displacement

the maximum top displacements are similar for most of the earthquakes, for a given amount of damping the $R_1$ values may vary significantly from one earthquake to another. This indicates that the nonlinear response of frames is highly sensitive to the time variation (frequency content) of ground motions. The dissipation of energy at PR connections is shown qualitatively in Fig. 5. The figure shows the moment and the corresponding rotation at a PR connection located in the left hand joint of Frame 1 for Earthquake 2, $T = 0.3$ and 2% damping. The area within the hysteresis loop represents the dissipation of energy at that particular connection.

To study the effect of the PR connection stiffness in dissipating energy, the same frame with a stiffer connection and a $T$ ratio of 0.6 is considered next. The fundamental period of the frame with this stiffer connection is found to be 0.42 sec. The frame is excited by the same earthquakes, and the results are shown in Table 4. In this case the frame developed plastic hinges for some earthquakes, and $E_P$ is calculated for those cases as shown in the table. For ease of discussion, two additional parameters $R_2$ and $R_3$ are introduced. $R_2$ represents the ratio of the energy dissipated at PR connections, $E_{C,}$ to that dissipated at plastic hinges, $E_P$, i.e., $R_2 = (E_C / E_P) \times 100$. $R_3$ represents the ratio of the energy dissipated at plastic hinges, $E_P$, to that dissipated by viscous damping, $E_D$, i.e., $R_3 = (E_P / E_D) \times 100$. The values of $R_2$ and $R_3$ are shown in Table 4.

The results in Table 4 confirm all the observations made in Table 3. If the frame undergoes significant deformation, the energy dissipated at PR connections is comparable to that dissipated by viscous damping. For low damping values, $E_C$ may be even larger than $E_D$. Three to five plastic hinges developed in the frame for Earthquakes 1, 3, 5 and 7. As expected, the $E_P$ values decrease as damping increases. $E_C$ is significantly larger than $E_P$ in most cases.

Comparing Table 3 ($T = 0.3$) and Table 4 ($T = 0.6$), it can be observed that $U_{\max}$ decreases as the stiffness of the connections increases for most of the earthquakes (Earthquakes 2, 3, 4, 6, 8, and 9). However, for Earthquakes 1, 5 and 7 and low values of damping, $U_{\max}$ increases as the connections become stiffer. The $R_1$ values, although still significant, decrease as the connection becomes stiffer. The results in Tables 3 and 4 indicate that, in most cases, the major source of energy dissipation is the hysteretic behavior at PR connections, particularly for low damping values.

Frame 1 with stiff connections ($T = 0.9$) is studied next. The fundamental period of the frame is found to be 0.4 sec. The results are summarized in Table 5. The results reconfirm the observations made earlier. $U_{\max}$ does not decrease as the frame becomes stiffer in all cases. For Earthquakes 3 and 5 and $\xi = 1\%$ damping, the frame develops a collapse mechanism due to excessive lateral displacement. Plastic hinges form at all beam-ends and at the bottom of columns. Thus, the seismic behavior of a frame with connections of intermediate stiffness may behave favorably compared to the frame with very stiff connections. For most cases, $E_P$ increases with an increase in the connection stiffness. The $R_1$ values decrease significantly as the $T$ ratio increases.

From a practical point of view, a connection with a $T$ ratio of at least 0.9 is considered to be a fully restrained (FR) connection, enabling the use of simpler analysis techniques. In order to estimate the error introduced by this simplified assumption, the same frame with FR connections ($T = 1.0$, no relative rotations between the beams and columns) is considered next. In this case, $E_C$, and thus $R_1$ and $R_2$ cannot be calculated.

The results are summarized in Table 6. Comparing Tables 5 and 6, it is observed that the energy dissipation behavior is quite different for the frame with PR and FR connections. The same observation can be made for the maximum base shear calculation as shown below. $U_{max}$ values decrease for the frame with FR connections in most cases. However, it becomes larger for Earthquakes 4, 7 and 9 and low damping values. For Earthquake 7 and $\xi = 1\%$, the frame develops a collapse mechanism, but it was stable when $T$ was 0.9. In general, the major source of energy dissipation for frames with stiffer

Table 8 Base shear for Frame 2 and different connection stiffness

| Earth. (1) | $\xi$ (%) (2) | $V_3$ (kN) (3) | $V_6$ (kN) (4) | $V_9$ (kN) (5) | $V_{FRC}$ (kN) (6) | $R_4$ (%) (7) | $R_5$ (%) (8) | $R_6$ (%) (9) |
|---|---|---|---|---|---|---|---|---|
| 1 | 1 | 575 | 723 | 972 | ** | 25.7 | 68.9 | ** |
| | 2 | 542 | 681 | 926 | 1,046 | 25.5 | 70.9 | 92.9 |
| | 5 | 449 | 562 | 699 | 794 | 25.3 | 55.8 | 77.0 |
| | 10 | 364 | 445 | 535 | 612 | 22.5 | 47.1 | 68.2 |
| 2 | 1 | 351 | 300 | 278 | 322 | -14.6 | -20.8 | -8.2 |
| | 2 | 345 | 295 | 276 | 299 | -14.4 | -19.8 | -13.4 |
| | 5 | 327 | 284 | 270 | 267 | -13.0 | -17.3 | -18.4 |
| | 10 | 302 | 269 | 258 | 250 | -10.8 | -14.5 | -17.1 |
| 3 | 1 | 840 | 687 | 740 | 1,063 | -18.2 | -11.9 | 26.5 |
| | 2 | 782 | 629 | 698 | 778 | -19.6 | -10.8 | -0.5 |
| | 5 | 648 | 490 | 586 | 627 | -24.3 | -9.5 | -3.2 |
| | 10 | 491 | 392 | 465 | 498 | -20.0 | -5.3 | 1.4 |
| 4 | 1 | 351 | 549 | ** | ** | 56.2 | ** | ** |
| | 2 | 341 | 553 | 930 | ** | 62.1 | 172.5 | ** |
| | 5 | 311 | 533 | 881 | 1,041 | 71.0 | 182.5 | 233.9 |
| | 10 | 279 | 505 | 747 | 872 | 80.7 | 167.1 | 211.6 |
| 5 | 1 | 416 | 370 | 563 | 527 | -11.1 | 35.3 | 26.7 |
| | 2 | 384 | 344 | 458 | 473 | -10.5 | 19.4 | 23.1 |
| | 5 | 315 | 271 | 341 | 360 | -14.0 | 8.2 | 14.2 |
| | 10 | 240 | 244 | 280 | 294 | 1.9 | 17.0 | 22.5 |
| 6 | 1 | 456 | 317 | 404 | 521 | -30.4 | -11.3 | 14.2 |
| | 2 | 375 | 288 | 349 | 403 | -23.1 | -6.7 | 7.7 |
| | 5 | 268 | 241 | 278 | 278 | -9.9 | 3.9 | 3.7 |
| | 10 | 207 | 229 | 245 | 251 | 10.6 | 18.3 | 21.3 |
| 7 | 1 | 466 | 548 | 843 | 955 | 17.6 | 80.8 | 104.9 |
| | 2 | 446 | 515 | 728 | 902 | 15.5 | 63.2 | 102.3 |
| | 5 | 395 | 487 | 541 | 641 | 23.3 | 36.7 | 62.0 |
| | 10 | 335 | 393 | 403 | 416 | 17.4 | 20.5 | 24.2 |
| 8 | 1 | 599 | 670 | 565 | 658 | 11.8 | -5.7 | 9.8 |
| | 2 | 541 | 568 | 542 | 627 | 4.9 | 0.2 | 15.8 |
| | 5 | 467 | 526 | 520 | 591 | 12.6 | 11.3 | 26.5 |
| | 10 | 383 | 432 | 476 | 498 | 12.7 | 24.1 | 29.9 |
| 9 | 1 | 377 | 364 | 369 | 440 | -3.6 | -2.3 | 16.6 |
| | 2 | 356 | 344 | 356 | 409 | -3.5 | -0.1 | 14.8 |
| | 5 | 311 | 325 | 338 | 364 | 4.5 | 8.5 | 17.0 |
| | 10 | 297 | 329 | 324 | 333 | 10.9 | 9.3 | 12.3 |

** = developed large lateral displacement

Table 9 Base shear for Frame 3 and different connections stiffness

| Earth. (1) | $\xi$ (%) (2) | $V_3$ (kN) (3) | $V_6$ (kN) (4) | $V_9$ (kN) (5) | $V_{FRC}$ (kN) (6) | $R_4$ (%) (7) | $R_5$ (%) (8) | $R_6$ (%) (9) |
|---|---|---|---|---|---|---|---|---|
| 1 | 1 | 623 | 921 | 1,415 | 1,526 | 47.9 | 127.1 | 145.0 |
| | 2 | 596 | 881 | 1,283 | 1,388 | 47.8 | 115.3 | 132.8 |
| | 5 | 538 | 801 | 1,001 | 1,072 | 48.8 | 86.0 | 99.2 |
| | 10 | 471 | 685 | 774 | 814 | 45.3 | 64.2 | 72.6 |
| 2 | 1 | 360 | 760 | ** | ** | 111.1 | ** | ** |
| | 2 | 347 | 747 | 1,143 | ** | 115.4 | 229.5 | ** |
| | 5 | 338 | 703 | 1,082 | 1,357 | 107.9 | 220.1 | 301.3 |
| | 10 | 324 | 614 | 796 | 1,246 | 89.0 | 145.2 | 283.6 |
| 3 | 1 | 965 | 1,210 | ** | ** | 25.4 | ** | ** |
| | 2 | 956 | 1,099 | ** | ** | 14.9 | ** | ** |
| | 5 | 836 | 845 | 1,038 | 1,375 | 1.1 | 24.2 | 64.4 |
| | 10 | 729 | 738 | 860 | 1,050 | 1.2 | 17.9 | 43.9 |
| 4 | 1 | 623 | 658 | 793 | ** | 5.7 | 27.4 | ** |
| | 2 | 614 | 627 | 681 | ** | 2.2 | 11.0 | ** |
| | 5 | 605 | 614 | 644 | 1,207 | 1.5 | 6.5 | 99.6 |
| | 10 | 578 | 600 | 638 | 1,172 | 3.9 | ** | 102.7 |
| 5 | 1 | 422 | 979 | 422 | 719 | 131.6 | 0.0 | 70.2 |
| | 2 | 378 | 832 | 379 | 645 | 120.0 | 0.4 | 70.6 |
| | 5 | 329 | 712 | 331 | 491 | 116.2 | 0.7 | 49.3 |
| | 10 | 324 | 605 | 327 | 400 | 86.3 | 1.0 | 23.4 |
| 6 | 1 | 689 | 1,348 | 687 | 896 | 95.5 | -0.3 | 29.9 |
| | 2 | 671 | 1,143 | 670 | 691 | 70.2 | -0.2 | 3.0 |
| | 5 | 672 | 867 | 672 | 476 | 29.1 | 0.0 | -29.1 |
| | 10 | 601 | 734 | 601 | 431 | 22.1 | 0.0 | -28.2 |
| 7 | 1 | 490 | 671 | 920 | 656 | 36.9 | 87.6 | 33.8 |
| | 2 | 468 | 618 | 815 | 546 | 32.0 | 74.0 | 16.7 |
| | 5 | 418 | 547 | 649 | 384 | 30.8 | 55.2 | -8.0 |
| | 10 | 372 | 480 | 509 | 249 | 28.9 | 36.6 | -33.1 |
| 8 | 1 | 821 | 1,277 | ** | ** | 55.5 | ** | ** |
| | 2 | 789 | 1,148 | ** | 1,139 | 45.4 | ** | 44.3 |
| | 5 | 741 | 1,010 | ** | 1,096 | 36.2 | ** | 47.8 |
| | 10 | 628 | 854 | 894 | 951 | 36.0 | 42.4 | 51.5 |
| 9 | 1 | 458 | 720 | ** | 545 | 57.3 | ** | 18.9 |
| | 2 | 404 | 649 | 1,004 | 504 | 60.4 | 148.0 | 24.5 |
| | 5 | 311 | 542 | 864 | 447 | 74.3 | 177.4 | 43.7 |
| | 10 | 277 | 422 | 681 | 414 | 52.2 | 145.4 | 49.2 |

** = developed large lateral displacement

connections is damping, particularly when it is high. In order to minimize the inaccuracies in the analysis procedure, at least for nonlinear seismic analysis, a connection with a $T$ ratio of at least 0.9 should not be considered to be FR type. It should be modeled as PR connection.

Finally, the effect of the PR connection stiffness on the overall seismic response is studied in terms of the maximum total base shear. The results are shown in Table 7 for Frame 1. $V_3$, $V_6$, $V_9$, and $V_{FRC}$ represent the maximum base shear when the $T$ ratio is 0.3, 0.6, 0.9, and 1.0, respectively. For ease of discussion, three additional parameters, $R_4$, $R_5$ and $R_6$, are introduced. They are defined as $R_4 = (V_6 - V_3) / V_3 \times 100$, $R_5 = (V_9 - V_3) / V_3 \times 100$, and $R_6 = (V_{FRC} - V_3) / V_3 \times 100$. Positive values of these parameters imply that the base shear is higher compared to the case when the $T$ ratio is 0.3.

The results in Table 7 indicate that the values of $R_4$, $R_5$ and $R_6$ are positive for many cases, implying that the maximum total base shear increases as the connection stiffness increases. Even when negative values occur for $R_4$, $R_5$ and $R_6$, they are smaller in magnitude than the positive values.

Frames 2 and 3 are analyzed similarly and tables similar to Tables 3 through 7 are developed. They cannot be shown here due to lack of space. The observations made for Frame 1 are also valid for these frames. The only additional observation is that the $R_1$ values increase with the height of the frames, indicating that PR connections dissipate more energy than viscous damping for taller frames. For $T$ = 0.3, the $R_1$ parameter ranges from 8.77 to 516.09% for Frame 2 and from 10.36 to 929% for Frame 3.

The information on the maximum base shear for Frames 2 and 3 are summarized in Tables 8 and 9, respectively. By comparing Tables 7, 8 and 9, it is observed that for most earthquakes, the maximum base shear increases with the stiffness and height of the frames.

In general, it can be concluded that the maximum total base shear may increase significantly as the connection stiffness increases. On the other hand, the maximum top lateral displacement does not always increase as the connections become more flexible, as expected for static application of the load. Even though the stiffness of the frame with PR connections is lower than that of the frame with FR connections, the response under earthquake loading depends largely on the dynamic characteristics of both the frame and the earthquake excitation. Thus, it may be beneficial to use PR frames as opposed to FR frames for seismic loading since they dissipate more energy, develop less base shear and may not produce large lateral deformation, provided that stable hysteretic behavior of the PR connections develops. This study analytically confirms some of the recent laboratory observations.

## 7. Conclusions

The major sources of energy dissipation in steel frames with partially restrained (PR) connections subjected to seismic loading are studied. A nonlinear seismic response algorithm developed and implemented by the authors is used to quantify major sources of energy dissipation. Available experimental results are used to verify the algorithm. The verified model is then used to quantify the energy dissipation due to viscous damping and the hysteretic behavior of the material at PR connections, and at plastic hinges if they form. Three steel frames, representing different dynamic characteristics with three different connection stiffnesses, are excited by several recorded earthquakes. Different sources of energy dissipation, lateral deformation and base shear are calculated for each case. In general, the analytical study confirms the behavior observed during experimental investigation: PR connections reduce the overall stiffness of frames, but add a major source of energy dissipation. The dissipation at PR connections is comparable to and may be even greater than that from viscous damping and at plastic hinges. This is particularly important if the connections are very flexible.

In general, the maximum total base shear may significantly increase as the connections stiffness increases. The increase tends to be larger for taller frames. On the other hand, the maximum top lateral displacement, $U_{max}$, does not always increase with a decrease in the connection stiffness. Even though the stiffness of the frame with PR connections is lower than that of the frame with FR connections, the response under earthquake loading largely depends on the dynamic characteristics of both the structure and the earthquake excitation. Thus, frames with PR connections may behave favorably compared to the frames with FR connections provided that stable hysteretic behavior of PR connections develops. The energy dissipation behavior for a frame with FR connections and a $T$ ratio of 1.0 is different than when the $T$ ratio of 0.9. Thus, for nonlinear seismic analysis, a $T$ ratio of at least 0.9 should not be considered to be an FR connection.

The study numerically confirms the general observations made in experimental results for frames with PR connections. Proper consideration of the stiffness of PR connections and other dynamic properties is essential to predict dynamic behavior. Modeling the connection behavior as realistically as possible in terms of its stiffness and damping characteristics is essential, no matter how difficult the analysis procedure becomes. Any simplified approach may need to be calibrated using this type of detailed analytical study.

## Acknowledgements

This paper is based on work partly supported by the National Science Foundation under Grant CMS-9526809. The work is also partially supported by El Consejo Nacional de Ciencia y Tecnologia (CONACyT), México under Grant 486100-5-28464U, and by La Universidad Autónoma de Sinaloa (UAS), México. Any opinions, findings, conclusions or recommendations expressed in this publication are those of the authors and do not necessarily reflect the views of the sponsors.

## References

American Institute of Steel Construction (1994), *Manual of Steel Construction: Load and Resistance Factor Design*, Chicago, Illinois.

Clough, R.W., Penzien, J. (1993), *Dynamics of Structures*, 2nd edition. New York: McGraw-Hill.

Disque, R.O. (1964), "Wind connections with simple framing", *Eng. J.*, AISC **1**(3), 101-3.

Elnashai, A.S., Elghazoulli, A.Y. and Denesh-Ashtiani, F.A. (1998), "Response of semi-rigid steel frames to cyclic and earthquake loads", *J. Struct. Eng.*, ASCE **124**(8), 857-867.

Gao, L. and Haldar, A. (1995), "Safety evaluation of frames with PR connections", *J. Struct. Eng.*, ASCE **121**(7), 1101-1109.

Haldar, A. and Nee, K.M. (1989), "Elasto-plastic large deformation analysis of PR steel frames for LRFD", *Comput. and Struct.* **31**(5), 811-823.

Jayakumar, P. and Beck, J.I. (1988), "System identification using nonlinear structural models", *Structural Safety Evaluation Based on System Identification Approaches*, H.G. Natge and J.T.P. Yao (Eds.), Vieweg & Sons, Wiesbaden, Germany.

Leon, R.T. and Shin, K.J. (1995), "Performance of semi-rigid frames", *Proc. of Structure Congress* 1020-1035.

Nader, M.N. and Astaneh, A. (1991), "Dynamic behavior of flexible, semirigid and rigid frames", *J. Constr. Steel Res.* **18**, 179-192.

Reyes-Salazar, A. (1997), "Inelastic seismic response and ductility evaluation of steel frames with fully, partially restrained and composite connections", PhD. Thesis, Department of Civil Engineering and Engineering Mechanics, University of Arizona, Tucson, AZ.

Reyes-Salazar, A. and Haldar, A. (2000), "Dissipation of energy in steel frames with PR connections", *Struct. Eng. and Mech., An Int. J.* **9**(3), 241-256.
Richard, R.M. (1993), "PRCONN, moment-rotation curves for partially restrained connections", RMR Design Group, Tucson, Arizona.
Richard, R.M., Allen, J., Partridge, J.E. (1997), "Proprietary slotted beam connection designs", *Modern Steel Construction*, AISC 28-33.
Roeder, C.W., Schneider, S.P., Carpenter, J.E. (1993), "Seismic behavior of moment-resisting steel frames: analytical study", *J. Struct. Eng.*, ASCE **119**, 1866-1884.
Shi, G. and Atluri, S.N. (1998), "elasto-plastic large deformation analysis of space-frames", *Int. J. Numer. Meth. Eng.*, **26**, 589-615.
Uang, C.M., Bertero, V.V. (1990), "Evaluation of seismic energy in structures", *J. Earthq. Eng. and Structural Dynamics* **19**, 77-90.
*CU*